MADRID
inter.noise 2019
June 16 - 19
NOISE CONTROL FOR A BETTER ENVIRONMENT

Estimation of normal incidence sound absorption coefficient of porous asphalt mixture by its porosity and the new particle distribution index

Park, Hee Jin [1]
Technical Research Laboratory, Nippon Road Co. Ltd.
2-11-20 Tamagawa, Ota-ku, Tokyo 146-0095, Japan

Iwai, Shigeo [2]
College of Science & Technology, Nihon University
1-10-2-701 Minamiyama, Shiroi, Chiba 270-1423, Japan

ABSTRACT

Porous asphalt pavement with a surface layer made by porous asphalt mixture (PAM) is widely prevalent to reduce tire/road noise. It is important to recognize an acoustic absorption effect of the surface layer (PAM medium) without its direct measurement at the design stage before construction of the pavement. The acoustic absorption effect of PAM medium is usually evaluated by the normal incidence sound absorption coefficient (NISAC). In this paper, firstly, approximate expressions which are transcribed the phenomenological absorber model derived by Hamet et al with the porosity of PAM medium as a variable is derived for evaluating the NISAC of PAM medium. Then, it is shown that the NISAC of PAM medium can be estimated by only two factors, the targetry porosity and the thickness of PAM medium without its direct measurement. Secondly, the PDI is calculated by geometry of the particle size distribution compatible with the targetry porosity and the $\overline{\text{NISAC}}$ is obtained by the ratio of the area of the NISAC zone of PAM medium to the area of the complete absorption coefficient zone in the figure of the relationship between frequency and the NISAC in the certain frequency period are proposed for the quantitative evaluation of the NISAC of PAM medium. From the result of considerations of the relationship between the PDI and the$\overline{\text{NISAC}}$, it is clear that the NISAC of PAM medium can quantitatively evaluate by the PDI and the $\overline{\text{NISAC}}$ at the design stage.

Keywords: Absorption, Pavement, Material
I-INCE Classification of Subject Number: 35

1. INTRODUCTION

Porous asphalt pavement is widely prevalent to reduce tire/road noise. Porous asphalt mixture (PAM) medium with large and contiguous air voids is set on the top of the pavement as an absorbing layer of noise. The aggregate mix proportion of PAM is

[1] hijin.paku@nipponroad.co.jp
[2] iwais@leaf.ocn.ne.jp

different from the aggregate mix proportion of ordinary dense asphalt mixture. These air voids is made by reducing amount of fine aggregates in the particle size range between 0.075mm and 5.0mm. Then, the air void is usually estimated by the porosity.

Figure 1 shows the typical aggregate mix proportion called as a particle size distribution of PAM[1]. The particle size distribution curve moves to lower area with increasing the porosity of PAM due to deducing amount of fine aggregates.

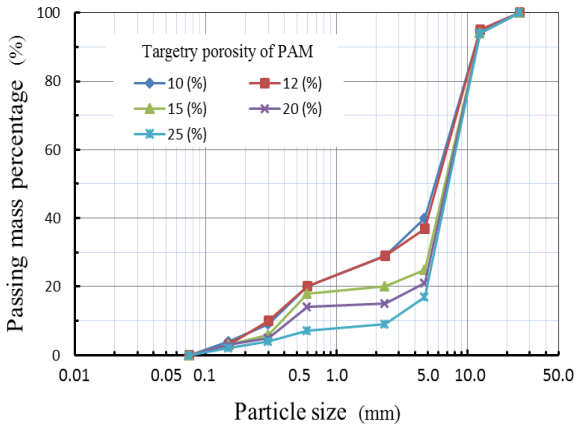

Figure 1 *Particle size distribution of PAM*[1]

The acoustic absorption effect of PAM medium is usually evaluated by the normal incidence sound absorption coefficient (NISAC). Then, many properties and factors are intricately related to its NISAC. Figure 2 shows the estimation flow chart of the NISAC of PAM medium and the correlation among materials, procedure, and the physical/acoustical properties and factors affected to its NISAC. After the selection of the suitable particle size distribution for the targetry porosity, PAM medium is made by the way which prepared aggregates and asphalt are mixed together and compacted. In this process, large and contiguous air voids are formed in PAM medium and generate the some physical/acoustical properties and factors affected to its NISAC.

By the way, at the design stage before construction of the pavement, it is important to recognize the NISAC of PAM medium without its direct measurement. In past years, two prediction models for the NISAC of PAM medium had been proposed. One is the phenomenological absorber model which had been derived by von Meier[2] and Hamet[3], other is the microstructural absorber model which had been derived by Attenborough and Howoth[4]. These models are consisted by the physical/acoustical factors which are obtained by direct and indirect measurement, as shown in Figure 2.

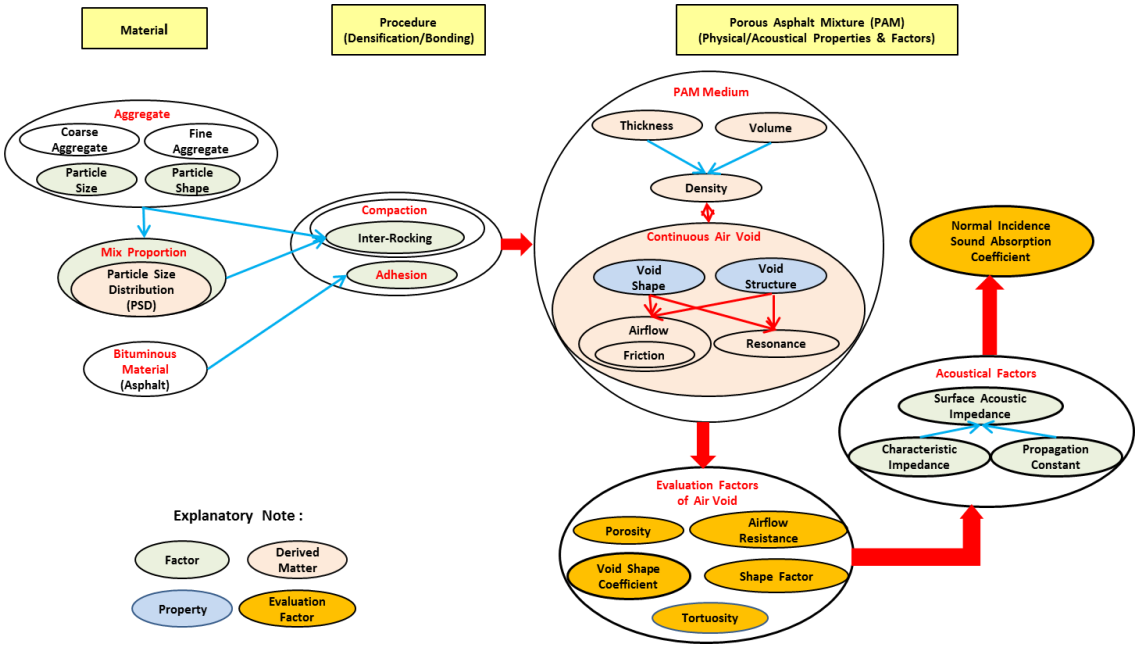

Figure 2 *Estimation flow chart of NISAC of PAM medium and correlation among materials, procedure, and the physical/acoustical properties and factors*

Then, the NISAC predicted by the both models is usually shown as the qualitatively-described result such as a figure of the relationship between frequency and the NISAC. However, it is hard to estimate the NISAC of PAM medium without direct measurement values of its physical/acoustical factors at the design stage, and also it is hard to compare quantitatively each qualitatively-described result of different kinds of PAM medium.

In this paper, firstly, after discussion of the correlation among the specific air flow resistance, the shape factor and the porosity of PAM medium, it is considered the possibility that approximate expressions which are transcribed the phenomenological absorber model derived by Hamet et al[3), 6)] with the porosity of PAM medium as a variable is derived for evaluating the NISAC of PAM medium.

Secondly, the objective evaluation of the NISAC of PAM medium reflecting the particle size distribution is considered. For this consideration, two new evaluation indexes are proposed. One is a new particle distribution index (PDI) which is calculated by geometry of the particle size distribution compatible with the targetry porosity. Other is the frequency averaged NISAC ($\overline{\mathrm{NISAC}}$) which is obtained by the ratio of the area of the NISAC zone of PAM medium to the area of the complete absorption coefficient zone in the figure of the relationship between frequency and the NISAC in the certain frequency period. Then, it is also considered the possibility that the NISAC of PAM is quantitatively estimated by the targetry porosity, the PDI and the $\overline{\mathrm{NISAC}}$ without direct measurement of the NISAC at the design stage.

These considerations are carried out based on both author's doctoral theses[1), 7)]. Therefore, almost every equations and figures are drawn from both theses.

2. NISAC ESTIMATION OF PAM MEDIUM BY APPROXIMATE EXPRESSION OF W^* AND γ^*

2.1 The correlation among airflow resistance, shape factor and porosity of void in PAM medium

2.1.1 Normal incidence sound absorption coefficient (NISAC) α and acoustic impedance Z of PAM medium

The normal incidence sound absorption coefficient (NISAC) α is given as follows for sound absorbing materials[5)].

$$\alpha = 1 - \left|\frac{Z-\rho c}{Z+\rho c}\right|^2 \tag{1}$$

here, Z: acoustic impedance (kg/sm^2), ρ: density of air (kg/m^3),
c: acoustic velocity (m/s)

If PAM is putted on the base course of pavement as a surface layer, the acoustic impedance Z is written as follows[3), 6)],

$$Z = W\coth(\gamma e) \tag{2}$$

here, W: characteristic impedance (kg/sm^2), γ: propagation constant (rad/m),
e: thickness (m)

2.1.2 Characteristic impedance W and propagation constant γ by Hamet et al

Hamet et al have derived the characteristic impedance W and the propagation constant γ as follows[3), 6)] respectively,

$$W = \rho c \frac{\sqrt{K}}{\Omega}\sqrt{1 - i\cdot\frac{R_s\Omega}{\omega\rho K}} \tag{3}$$

$$\gamma = i \cdot \frac{\omega}{c}\sqrt{K}\sqrt{1 - i \cdot \frac{R_s \Omega}{\omega \rho K}} \qquad (4)$$

here, K: shape factor, Ω: porosity, R_s: specific airflow resistance (kNs/m^4)
ω: angular frequency (=2πf) (rad/s), f: frequency (Hz, 1/s)

2.1.3 Approximate expression of characteristic impedance W^* and propagation constant γ^* at 15℃[1)]

1) Relationship between porosity Ω and specific airflow resistance R_s

Figure 3 shows experimental data of the porosity Ω of PAM medium and its specific airflow resistance R_s with the different airflow velocity. The test specimens were made by the Marshall Test procedure applied by the particle size distribution shown in Figure 1. Between Ω and R_s, it is found to have a strong correlation. Under the low airflow velocity condition (v_a: 0.032-0.035(m/s)) like as the laminar flow condition, the both relationship can be expressed by a regression equation as follows,

$$R_s = 51.20 * \Omega^{-2.944} \quad (\mathrm{kNs/m^4}),\ (0.1 \le \Omega \le 0.31),\ (R^2 = 0.896) \qquad (5)$$

2) Relationship between porosity Ω and shape factor K

The shape factor K of PAM medium was calculated by a following equation which was rewritten the original equation proposed by Hamet et al[6)].

$$K = \left\{\frac{(2n+1)\cdot c}{f_{(2n+1)}\cdot 4e}\right\}^2 \qquad (n = 0,1,2,\cdots\cdots) \qquad (6)$$

here, $f_{(2n+1)}$: frequency (Hz) at the $(2n+1)^{\text{th}}$ peak absorption coefficient

Figure 4 shows the relationship between the porosity Ω of PAM medium and its shape factor K at a center frequency of a 1/3 octave band matched to the first peak absorption coefficient over 100Hz. The curve in the figure expresses the approximate relationship between Ω and K as the following Equation (7),

$$K = 2.077 * 10^{(0.02863/(\Omega - 0.07))} \quad (0.1 \le \Omega \le 0.31),\ (\text{central error: } 0.40) \qquad (7)$$

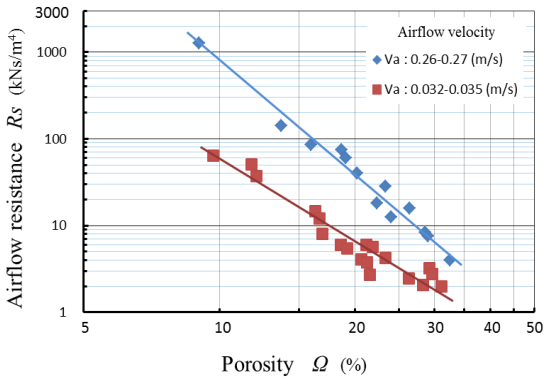

Figure 3 *Relationship between porosity Ω and specific airflow resistance R_s*[1)]

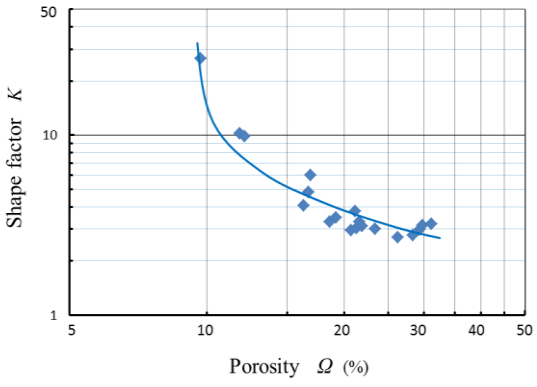

Figure 4 *Relationship between porosity Ω and shape factor K*[1)]

3) Approximate expression of characteristic impedance W^* and propagation constant γ^* at 15℃

The characteristic impedance W^* and the propagation constant γ^* at the atmosphere temperature 15℃ can be written as the following approximate expressions, as following

Equation (8), by an application of both Equation (5) and Equation (6), and the density of air $\rho = 1.222\ (\mathrm{kg/m^3})$ and the acoustic velocity $c = 340\ (\mathrm{m/s})$ at 15℃ to Equation (3) and Equation (4). Then, these are able to estimate by the porosity Ω of PAM medium at the required frequency.

$$\left.\begin{aligned} W^* &= \frac{598.796}{\Omega} * \sqrt{A - \frac{B}{f}\cdot i} \\ \gamma^* &= 0.02663 * f * \sqrt{-A + \frac{B}{f}\cdot i} \\ A(=K) &= 2.077 * 10^{(0.02863/(\Omega - 0.07))} \\ B &= 3.210 * \Omega^{-1.944} \end{aligned}\right\} \quad ((0.1 \le \Omega \le 0.31),\ \text{at } 15℃) \qquad (8)$$

2.2 Estimation of NISAC α of PAM by porosity Ω and thickness e at 15℃

Figure 5 - Figure 8 show the typical approximate results of the NISAC α (red-colored curves) at 15℃ estimated by the use of the approximate Equation (8), Equation (1) and Equation (2) with the theoretical curves of the NISAC α (blue-colored dot curves) calculated by Equation (3) and Equation (4) proposed by Hamet et al[6] and measured data α (black-colored dots) in response to the center frequency of the 1/3 octave band. In this calculation, the measured R_s value and K value are applied to Equation (3) and (4). Furthermore, Table 1 shows the comparisons of the measured values of R_s and K with the approximate values of R_s and K calculated by Equation (6) and (7), respectively.

A comparison of the approximate results with the theoretical curves by Equation (3) and (4) shows the same tendency, relatively in these figures. Then, as Hamet et al were

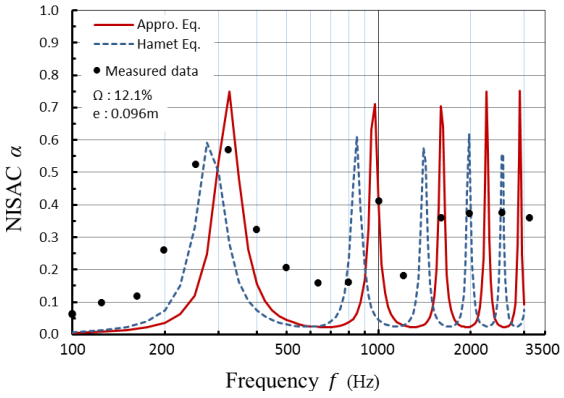

Figure 5 *Relationship between frequency f and NISAC α (Ω:12.1%)*

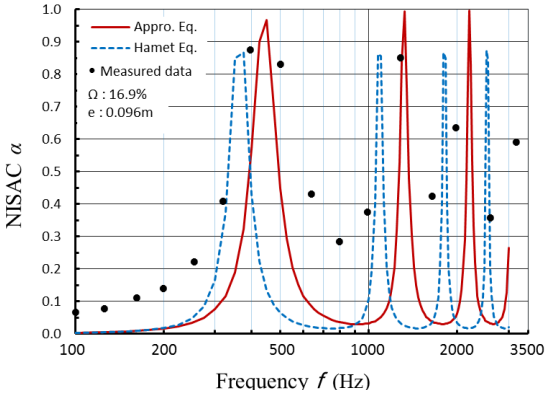

Figure 6 *Relationship between frequency f and NISAC α (Ω:16.9%)*

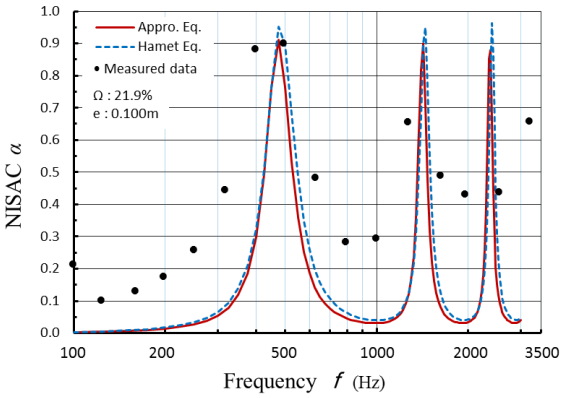

Figure 7 *Relationship between frequency f and NISAC α (Ω:21.9%)*

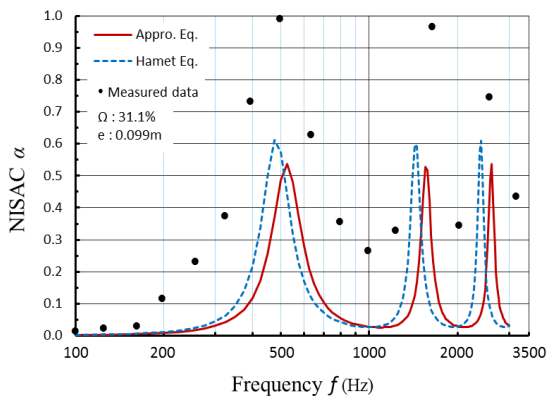

Figure 8 *Relationship between frequency f and NISAC α (Ω:31.1%)*

pointed out[6], the increase of R_s tends to decrease the peak the NISAC α, and also the increase of K tends to move the frequency at the peak NISAC α toward the lower frequency area.

Table 1 *Comparison of the measured values with the approximate values of R_s and K*

Porosity Ω		12.1 (%)	16.9 (%)	21.9 (%)	31.1 (%)
Specific airflow resistance R_s (kNs/m^4)	Measured value	36.97	8.05	5.66	1.97
	Approximate value	25.68	9.60	4.48	1.59
Shape factor K	Measured value	9.86	5.97	3.13	3.22
	Approximate value	7.57	4.04	3.23	2.73

In addition, a comparison of the both curves with the measured data of the NISAC α shows some differences. Particularly, the minimum values of the NISAC α in the each estimated curves deviate from the measured data. These results suggest that it is important to improve in accuracy of experiments and to recognize the application rage of the theoretical and approximate model. Especially, it is hard to determine the K value under limited data of the NISAC α at the center frequency of the 1/3 octave band.

2.3 Summary

(1) The porosity Ω of PAM medium has an influence on its specific air-flow resistance R_s and shape factor K, strongly. Then, approximate expression of R_s and K is obtained as a function of the porosity Ω, respectively.

(2) The approximate expression of the characteristic impedance W^* and the propagation constantγ^*at 15℃ is obtained by transcribing the phenomenological absorber model applied the approximate expression of R_s and K, as the function of the porosity Ω, respectively.

(3) If the targetry porosity Ω and the thickness e of PAM medium are set up, its NISAC α can be estimated by the use of Equation (1), (2) and (8) at the required frequency.

(4) There are some differences between the measured data and the estimated values by the phenomenological absorber model and the approximate expression.

(5) The estimation of the shape factor K which is indirect measurement includes some error due to the test of the NISAC α by 1/3 octave band frequency.

(6) It is hard to compare the NISAC α of different kinds of PAM medium because the NISAC α is shown as the qualitative figure of the relationship between frequency and the NISAC α in general.

3. QUANTITATIVE ESTIMATION OF NISAC OF PAM MEDIUM BY MATERIAL PROPERTY[7]

3.1 Particle distribution index (PDI) of PAM

As shown in Figure 2 and the above discussions, the particle size distribution and the shape of aggregates affect to the formation of air void and its characteristics in PAM medium. The particle size distribution is usually described as the figure of the relationship between the particle size and the passing mass percentage (PSP), as shown in Figure 1. Then, the PSP is calculated based on the sieving test result of aggregates.

However, the accumulated remaining mass percentage (ARMP) is easy to intuitively recognize how many amounts of aggregates are remaining over the certain particle size of aggregate. The ARMP is obtained as follows,

$$ARMP = 100 - (PSP) \quad (\%) \tag{9}$$

here, PSP: passing mass percentage (%)

The typical ARMP distribution curve is shown in Figure 9 as a blue-colored line. The shape of the both distribution curves of the particle size distribution and the ARMP distribution curve is geometrically-similar except the ordinate axis scale is reverse.

The ARMP distribution curve has a distinctive trend which changes rapidly at the boundary between fine aggregates (0.075mm ≤ the particle size ≤ 5.0mm) and coarse aggregates (over than the particle size 5.0mm) because amount of fine aggregates are reduced. The geometrical characteristics of this distinctive curve are defined as the ratio of the area of fine aggregate zone under the curve to the area of coarse aggregate zone under the curve as shown in Figure 9. The ratio is called as the particle distribution index (PDI) and is defined as following Equation (10).

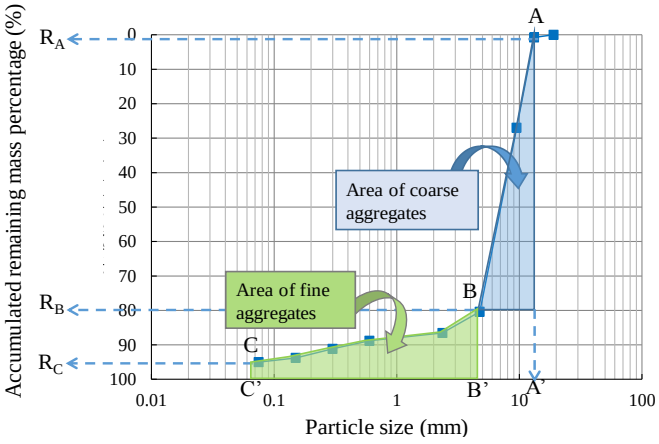

Figure 9 *Concept of PDI by ARMP distribution curve*[7)]

$$PDI = \frac{Area\ of\ fine\ aggregates}{Area\ of\ coarse\ aggregates} = \frac{BCC'B'}{ABB'A'} = \frac{\log(\frac{B'}{C'})}{\log(\frac{A'}{B'})} \times \frac{200-(R_C+R_B)}{(R_B-R_A)} \qquad (10)$$

here, R_A: ARMP at A'(%), R_B: ARMP at B' (%), R_C: ARMP at C' (%),
A': next lower open size from the sieve with the maximum mesh,
B': particle size of 5.0mm, C': particle size of 0.075mm

Evaluation possibility of the air void characteristics in PAM medium was discussed by checking for the correlation among the porosity Ω, the specific air-flow resistance R_s, and the PDI. Figure 10 shows the correlation between Ω and *PDI*. The porosity Ω decreases with decreasing the PDI, then the both relationship can be expressed by a regression equation with the high determination coefficient R^2 as follows,

$$\Omega = -13.847 * PDI + 32.188 \quad (\%), \qquad (R^2 = 0.975) \qquad (11)$$

Figure 11 shows the correlation between the specific air-flow resistance R_s, and the PDI. The specific air-flow resistance R_s rapidly increases with increasing the PDI.

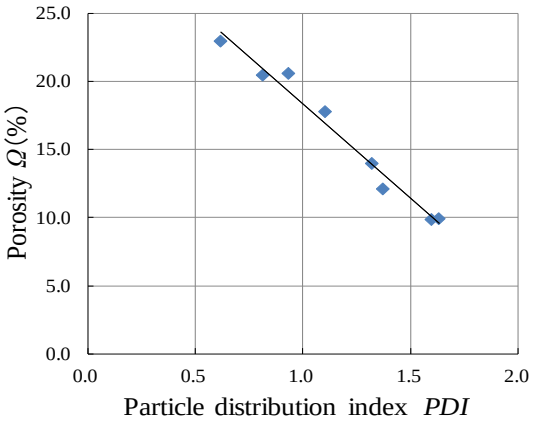

Figure 10 *Relationship between PDI and porosity* Ω[7)]

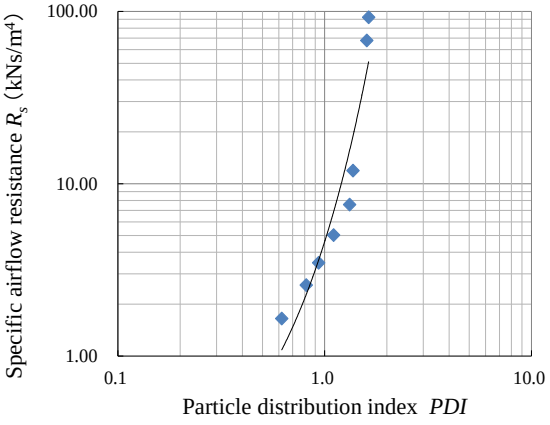

Figure 11 *Relationship between PDI and specific airflow resistance* R_s[7)]

The both relationship also can be expressed by a regression equation with the high determination coefficient R^2 as follows,

$$R_s = 0.1024 * exp(3.808 * PDI) \quad (\mathrm{kNs/m^4}), \quad (R^2 = 0.899) \qquad (12)$$

From the above discussion, it is clear that the PDI is the useful index for evaluating the air void characteristics in PAM medium.

3.2 Frequency averaged NISAC ($\overline{\mathbf{NISAC}}$) of PAM medium and its estimation by PDI

3.2.1 Frequency averaged NISAC ($\overline{\mathbf{NISAC}}$) of PAM medium

The other index is also discussed for the objective evaluation of the NISAC of PAM medium. The index is defined as the ratio of the area of the NISAC zone of PAM medium to the area of the complete absorption coefficient zone in the figure of the relationship between frequency and the NISAC in the certain frequency period. As the discussion result, the ratio is shown the frequency averaged NISAC of PAM medium, and is written as the$\overline{\mathrm{NISAC}}$.

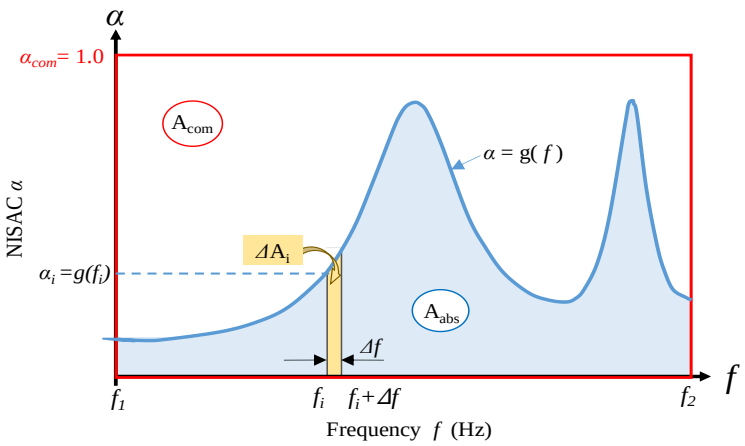

Figure 12 *Concept of absorption area A_{abs} and complete absorption area A_{com}*

Figure 12 shows the concept of the frequency averaged NISAC. When the NISAC α is a continuous function $g(f)$ as the frequency$f$, the area A_{abs} of the NISAC α in the certain frequency period $(f_1 \sim f_2)$ is written as follows,

$$A_{abs} = \lim_{\Delta f_i \to \infty} \sum_{i=1}^{n} g(f_i)\,\Delta f_i = \int_{f_1}^{f_2} g(f)df \qquad (13)$$

here, Δf_i: smallness interval of the continuous function $g(f)$ at f_i,
f_i: certain frequency (Hz), f_1: lower end frequency (Hz),
f_2: upper end frequency (Hz)

In case of$g(f) = \text{constant} = \alpha_{const}$ without relation to the frequency, the area A_{const} of the NISAC α is derived applying Equation (13) as follows,

$$A_{const} = \alpha_{const} \int_{f_1}^{f_2} df = \alpha_{const}(f_2 - f_1) \qquad (14)$$

here, α_{const}: certain constant value of the NISAC α

Then, in case of the complete absorption condition, the the area A_{const} of the NISAC α will become to the area A_{com} due to the constant value α_{const} will be $\alpha_{com} = 1.0$. Thus, the area A_{com} is written by Equation (14) as follows,

$$A_{com} = \alpha_{com} \int_{f_1}^{f_2} df = (f_2 - f_1) \quad (15)$$

here, α_{com} : constant value $(= 1.0)$ of the NISAC α at the complete absorption condition

Therefore, the ratio $(\overline{\text{NISAC}})$ of the area A_{abs} to the area A_{com} is written by applying Equation (13) and Equation (15) as follows,

$$\overline{NISAC} = \frac{A_{abs}}{A_{com}} = \frac{\int_{f_1}^{f_2} g(f)df}{\alpha_{com} \int_{f_1}^{f_2} df} = \frac{1}{(f_2 - f_1)} \int_{f_1}^{f_2} g(f)df \quad (16)$$

Thus, the $\overline{\text{NISAC}}$ means the frequency averaged area of NISAC of PAM medium as shown in Equation (16). Then, the frequency averaged area of PAM medium is called shortly as "frequency averaged NIST" or "$\overline{\text{NISAC}}$" in this paper.

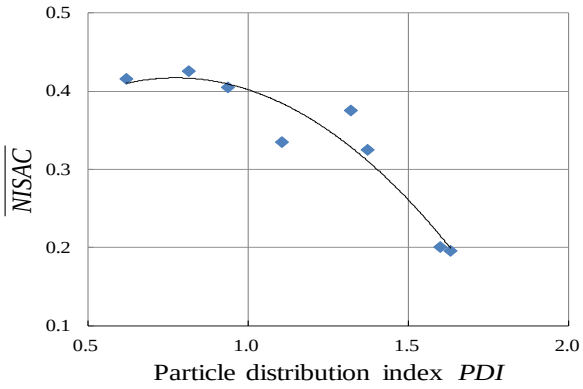

Figure 13 *Relationship between PDI and* $\overline{NISAC}$[7)]

Furthermore, the relationship between the PDI and the $\overline{\text{NISAC}}$ is considered. Figure 13 shows the correlation of between the PDI and the $\overline{\text{NISAC}}$ which are calculated by measured data. The both relationship can be expressed by a regression equation with the high determination coefficient R^2 as follows,

$$\left.\begin{array}{l} \overline{NISAC} = -0.297 * PDI^2 + 0.459 * PDI + 0.240 \quad (R^2 = 0.912), \\ (0.1 \leq \Omega \leq 0.25, \text{and the maximum aggregate size is under } 13mm) \end{array}\right\} \quad (17)$$

From the above consideration, it is clear that the PDI has a strong correlation with the $\overline{\text{NISAC}}$, and is the useful index for evaluating the $\overline{\text{NISAC}}$ of PAM medium.

3.2.2 Verification of compatibility between estimated $\overline{\text{NISAC}}$ and measured $\overline{\text{NISAC}}$

Compatibility of the estimated $\overline{\text{NISAC}}$ with the measured $\overline{\text{NISAC}}$ is verified. The estimated $\overline{\text{NISAC}}$ is calculated by the use of the other researcher's test data[8), 9), 10)], Equation (10), and Equation (17). Then, the measured $\overline{\text{NISAC}}$ is obtained by the other reseacher' data[8), 9), 10)] and Equation (16). The ARMP distribution curves for calculating the PDI are shown in Figure 14, all together.

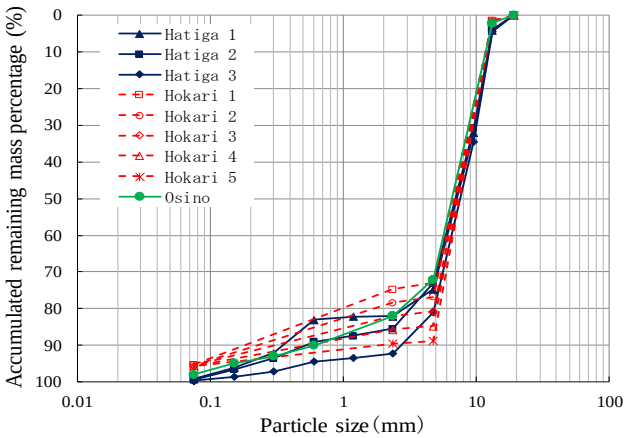

Figure 14 *Other researcher's ARMP distribution curve of PAM* [7)]

Figure 15 shows the both data of the average value of the measured

$\overline{\text{NISAC}}$ and the average value of the estimated $\overline{\text{NISAC}}$ for the PDI in a lump. The tendency of the $\overline{\text{NISAC}}$ decreases over-all with increasing the PDI in Figure 15 is almost the same tendency as shown in Figure 13.

Figure 16 shows over-all accuracy between the measured $\overline{\text{NISAC}}$ and the estimated $\overline{\text{NISAC}}$. Even though there are same scatterings, the estimated $\overline{\text{NISAC}}$ is in an error range of ±15% for the measured $\overline{\text{NISAC}}$. Therefore, it is clarified that the estimated $\overline{\text{NISAC}}$ has sufficient compatibility for the measured $\overline{\text{NISAC}}$.

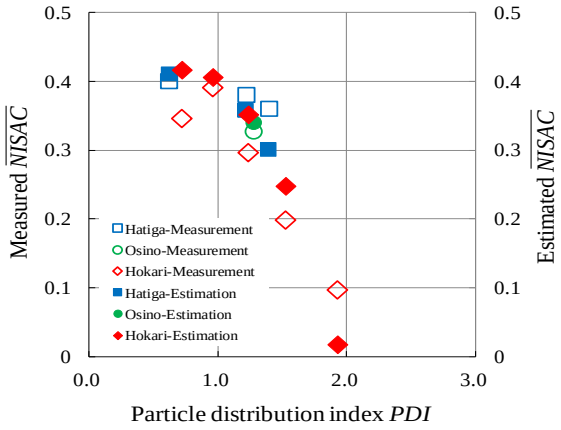

Figure 15 *Relationship among PDI, measured $\overline{NISAC}$ and estimated $\overline{NISAC}$*[7)]

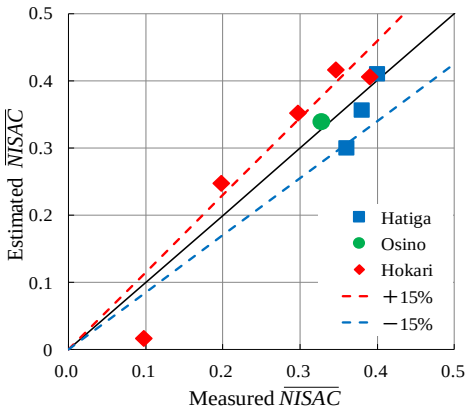

Figure 16 *Relationship between measured $\overline{NISAC}$ and estimated $\overline{NISAC}$*[7)]

3.3 Summary

(1) The particle size distribution of PAM is quantified by the particle distribution index (PDI) which is reflected the air void characteristics of PAM medium.

(2) The PDI has a strong correlation with the $\overline{\text{NISAC}}$ derived as the frequency averaged NISAC of PAM medium. Then, the acoustic absorption effect of PAM medium can be quantitatively evaluated by the both indexes, the PDI and the $\overline{\text{NISAC}}$.

(3) The estimated $\overline{\text{NISAC}}$ by the PDI has sufficient compatibility for the measured $\overline{\text{NISAC}}$ because the estimated $\overline{\text{NISAC}}$ is in an error range of ±15% for the measured $\overline{\text{NISAC}}$.

(4) The quantitative evaluation of the NISAC of PAM medium can be carried out by the use of the estimated $\overline{\text{NISAC}}$ calculated by the PDI for the certain particle size distribution.

(5) Thus, it is clear that the acoustic absorption effect of PAM medium can directly and quantitatively evaluate by material characteristics.

4. CONCLUSIONS

Two evaluation procedures of the NISAC of PAM medium by (1)approximate expressions as the function of its porosity Ω and thickness e, and (2)the PDI reflecting of its aggregate mix proportion and the frequency averaged NISAC ($\overline{\text{NISAC}}$) are proposed and discussed for clarifying their availability without direct measurement factors. Then, it is clear as follows,

(1) The NISAC of PAM medium can be estimated by the approximate expression of the characteristic impedance W and the propagation constant γ which are transcribed with the porosity Ω of PAM medium and its thickness e. However, it is hard to compare the NISAC of different kinds of PAM medium because the

NISAC is shown as the qualitative figure of the relationship between frequency and the NISAC, in general.

(2) If the targetry porosity of PAM medium is set up and chosen a suitable particle size distribution, the quantitative evaluation of the NISAC of PAM medium can be carried out by the use of the estimated $\overline{\mathrm{NISAC}}$ calculated by the PDI for the suitable particle size distribution, sufficiently.

(3) The quantitative evaluation for the NISAC of different kinds of PAM medium can be done by the estimated $\overline{\mathrm{NISAC}}$ without direct measurement of the NISAC at the design stage before construction of porous asphalt pavement.

5. ACKNOWLEGMENTS

Authors would like to extend our deep appreciations to the late Dr. Y. Miura (former NU,CST), Dr. S. Shimobe (NU,CST), Dr. J.F. Hamet (former INRETS), Dr. Y. Oshino (former JARI) and many cooperative former students of Nihon University, for their kind suggestions and supports.

REFFERENCES

1. S. Iwai, "*Study on tire/road noise reduction effect by porous asphalt pavement*", Doctoral thesis, Nihon University (in Japanese) (1998)
2. A. von Meier, "*A poro-elastic road surface for traffic noise reduction*", Proceedings of Inter-noise85 (1985)
3. J.F. Hamet, "*Modelisation acoustique dun enrobe drainant etude theoriqueen incidence normale*", Rapport INRETS n59 (1988)
4. K. Attenborough and C.Howorth, "Models for the acoustic characteristics of porous road surfaces", Proceedings of International Tire/Road Noise Conference (1990)
5. P. Morse and K. Ingard, "*Theoretical Acoustic*", McGraw-Hill, New York (1968)
6. M. Berengier, J.F. Hamet, and P. Bar, "*ACOUSTICAL PROPERTIES OF THE POROUS ASPHALT, THEORETICAL AND ENVIRONMENTAL ASPECT*", LCPC (1989)
7. H.J. Park, "*Study on evaluation and prediction of normal incidence sound absorption coefficient by the new granularity index of porous asphalt mixture*", Doctoral thesis, Nihon University (in Japanese) (2014)
8. K. Hokari, N. Hayashi, and Y. Matsumuro, "*Characteristic of normal incidence sound absorption coefficient of open-graded asphalt concrete*", Proceedings of 18th Japan Road Conference (in Japanese) (1989)
9. Y. Oshino, K. Tateishi, S. Osato, and M. Ozawa, "*Changes in automobile driving noise due to difference in road surface*", JARI Research Journal, No.13vol 3 (in Japanese) (1991)
10. A. Hachiga and K.Yoshikado, "*Study on the sound absorption coefficient of double-layered permeable asphalt mixture*", Undergraduate research papers, Nihon University, (in Japanese) (2008)